Supporting information

Engineering natural matrix with black phosphorus nanosheets to generate multi-functional therapeutic nanocomposite hydrogels†

Yali Miao,‡[ab] Xuetao Shi,‡[ab] Qingtao Li,[bc] Lijing Hao,[bc] Lei Liu,[ab] Xiao Liu,[ab] Yunhua Chen*[abd] and Yingjun Wang *[abde]

[a] School of Materials Science and Engineering, South China University of Technology, Guangzhou 510640, China. E-mail: msyhchen@scut.edu.cn

[b] National Engineering Research Center for Tissue Restoration and Reconstruction, South China University of Technology, Guangzhou 510006, China. E-mail: imwangyj@scut.edu.cn

[c] Key Laboratory of Biomedical Engineering of Guangdong Province, and Innovation Center for Tissue Restoration and Reconstruction, South China University of Technology, Guangzhou 510006, China

[d] Key Laboratory of Biomedical Materials and Engineering of the Ministry of Education, South China University of Technology, Guangzhou 510006, China

[e] Guangzhou Regenerative Medicine and Health Guangdong Laboratory, Guangzhou 510005, China.

‡ These authors contributed equally

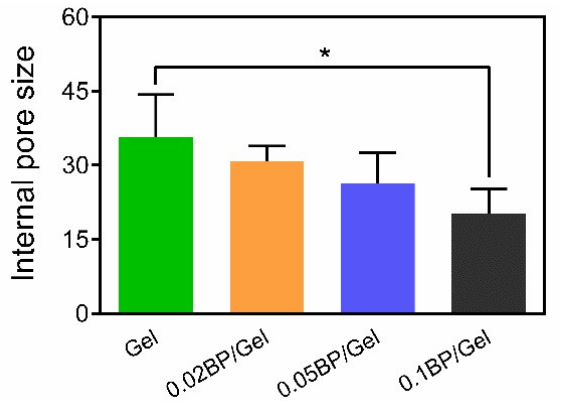

Fig. S1 Quantitative analysis of pore size inside composite hydrogels based on SEM images.

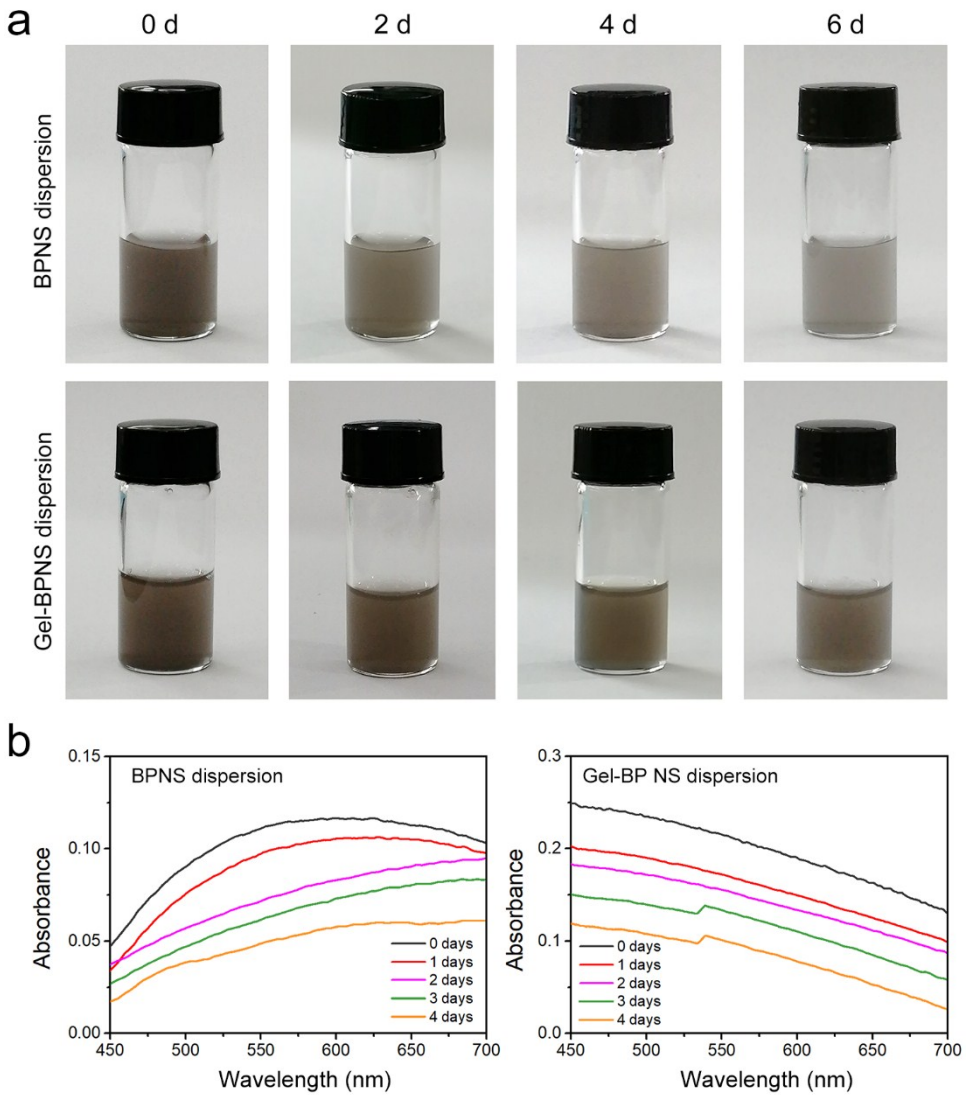

Fig. S2 The degradation of 0.02 w/v% BP nanosheets and 0.02 w/v% GelMA decorated BP nanosheets (Gel-BP). (a) The appearance of the aqueous dispersion of BP nanosheets and Gel-BP after 0, 2, 4 and 6 days of storage. (b) The UV-Vis absorption spectra of the aqueous dispersion of BP nanosheets and Gel-BP after 0, 1, 2, 3 and 4 days of storage.

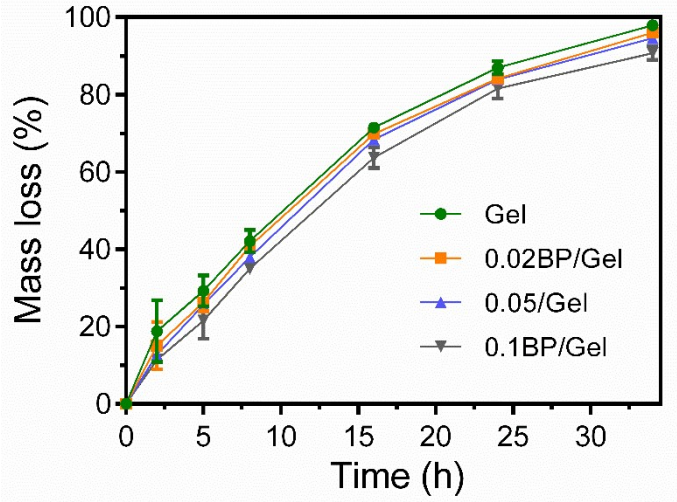

Fig. S3 Enzymatic degradation of the nanocomposite hydrogels with different concentrations of BP nanosheets in response to collagenase II (1 μg/mL).

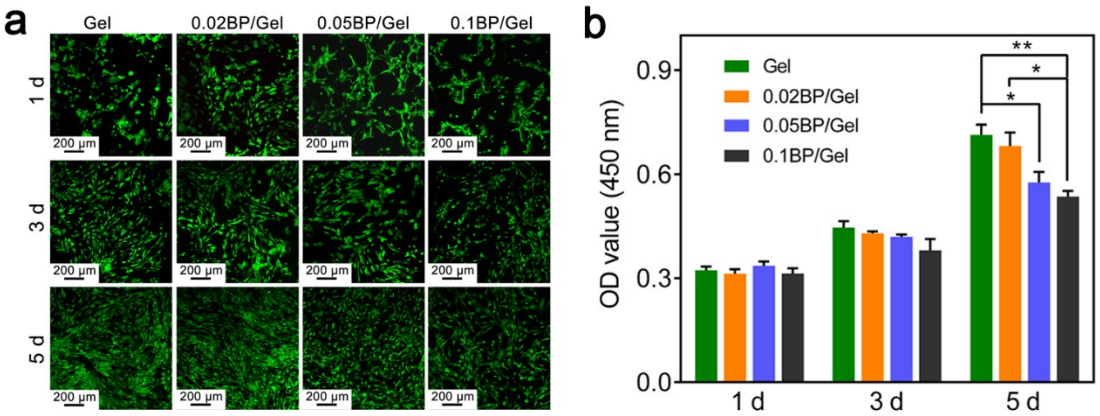

Fig. S4 *In vitro* cell viability of therapeutic nanocomposite hydrogels. (a) Fluorescence micrographs of hMSCs cultured on hydrogels on day 1, 3 and 5. The green represents the living cells, while the red represents dead cells. (b) Proliferation of hMSCs determined by CCK8 assay (*$p < 0.05$, **$p < 0.01$, ***$p < 0.001$).

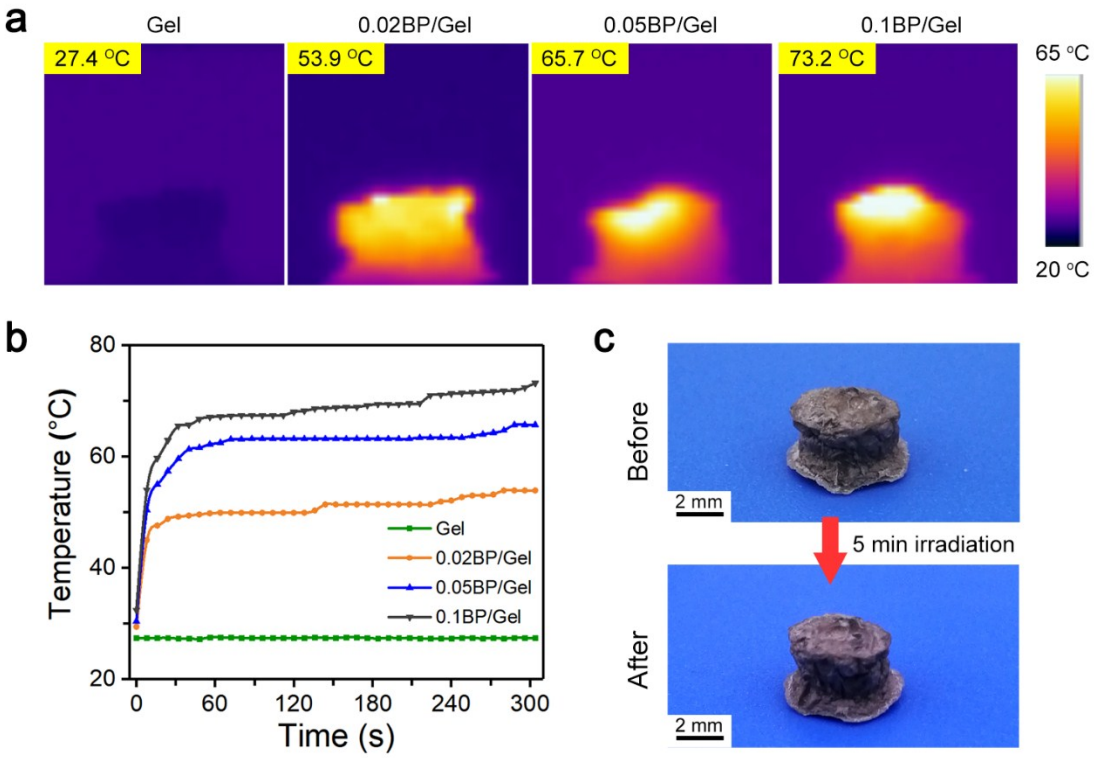

Fig. S5 (a) Infrared thermographic photographs of dried nanocomposite hydrogels irradiated by 808 nm NIR laser (1 W cm^{-2}). (b) Photothermal heating curves of the nanocomposites *in vitro* as a function of time. (c) Structural stability of dried nanocomposite hydrogel before and after NIR laser irradiation.

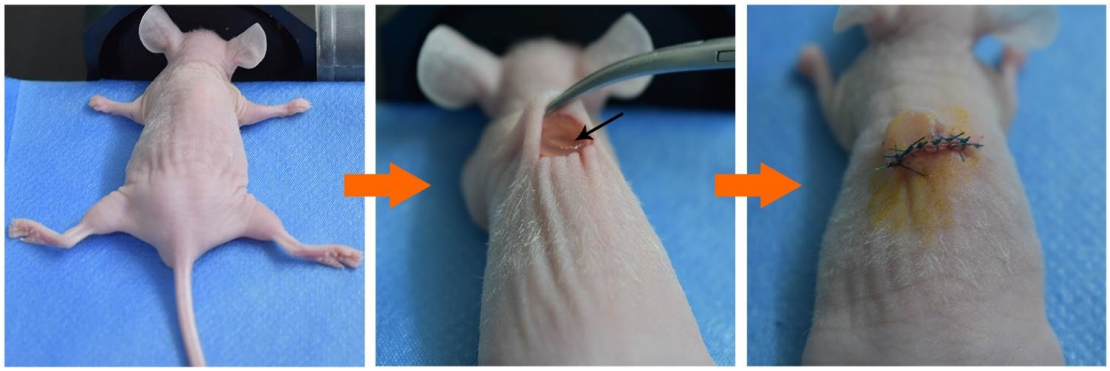

Fig. S6 Animal experimental process consists that the implantation process of therapeutic BP/Gel nanocomposite hydrogel in nude mice and the observation of implant in nude mice before tissue collecting.

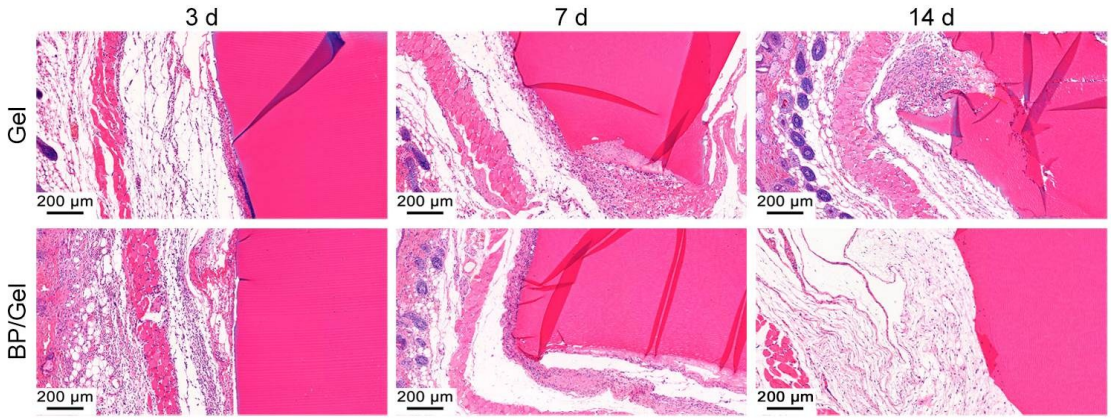

Fig. S7 HE staining results at specific time points after implantation in nude mice to evaluate the biocompatibility of the therapeutic BP/Gel nanocomposite hydrogel.

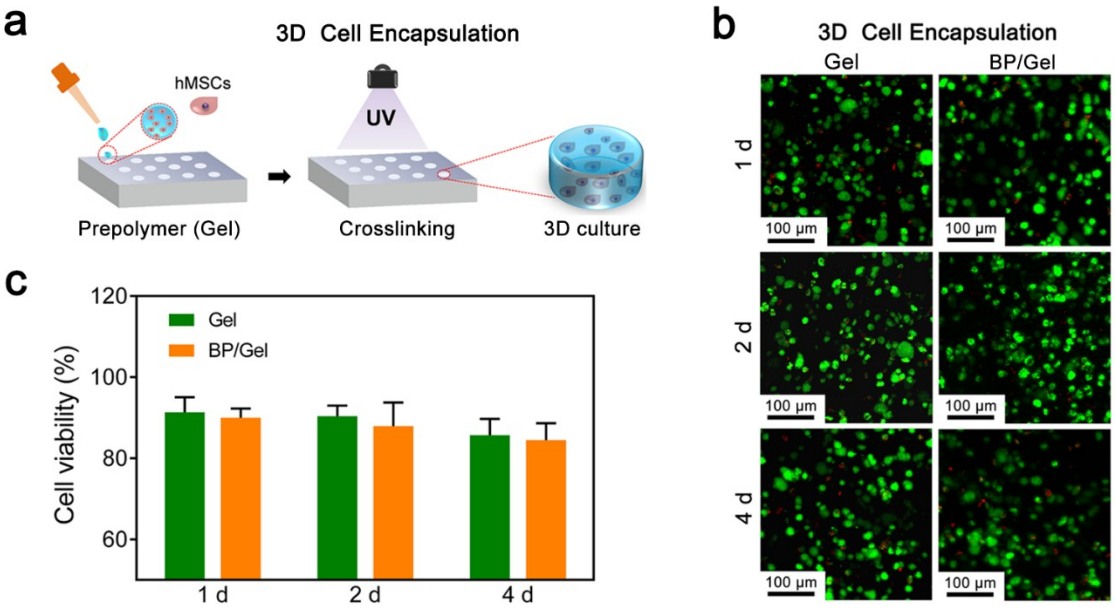

Fig. S8 (a) The schematic diagram of 3D Cell encapsulation in BP/Gel nanocomposite hydrogel. (b) Live/dead staining assay of hMSCs cells in gelatin and BP/Gel nanocomposite hydrogel, live cells: green fluorescence, dead cells: red fluorescence. (c) Fluorescence quantitative analysis of cell viability.

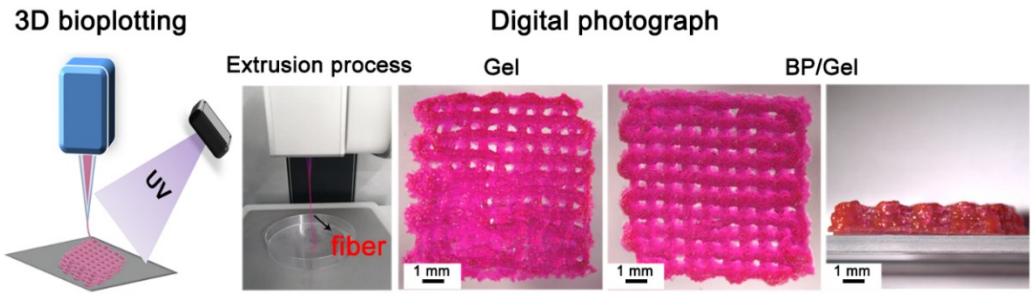

Fig. S9 3D printable demonstration of the therapeutic BP/Gel nanocomposite hydrogel. The addition of BP nanosheets shows great stability improvement of the hydrogel matrix after printing.